

Optomechanical Force Sensor in Non-Markovian Regime

Wen-Zhao Zhang¹, Yan Han², Biao Xiong¹, Ling Zhou^{1,*}

Abstract. The optomechanical force sensor in non-Markovian environment for a mechanical oscillator is presented. By performing homodyne detection, we obtain a generally expression for the output signal. It is shown that the weak force detection is sensitive to the non-Markovian environment. The additional noise can be reduced and the mechanical sensitivity can be obviously amplified in resolved sideband regime comparing to the Markovian condition without using assistant system or squeezing. Our results provide a promising platform for improving the sensitivity of weak force ultrasensitive detection.

¹ School of Physics and Optoelectronic Technology, Dalian University of Technology, Dalian 116024, People's Republic of China

² School of Physics and Optoelectronic Technology, Taiyuan University of Technology, Taiyuan 030024, People's Republic of China

* Author to whom any correspondence should be addressed.

E-mail: zh1hxn@dlut.edu.cn

February 2016

1. Introduction

Optomechanical systems provide us a platform for high precision measurements including ultra-sensitive force detection [1], small quantities of adsorbed mass detection [2] and low-reflectivity object detection [3]. Such systems exploit the huge susceptibility around the resonance frequency of oscillators with excellent mechanical quality factor Q_m , combined with high-sensitivity interferometric measurements [1, 4]. The photon shot noise in the optomechanical systems will broaden the optical response spectrum and finally affect the sensitivity of detection during the frequency measurement [5, 6], which means that the shot noise should be reduced. However, reduced shot noise would increase quantum back-action noise force due to the opposite scalings with the optical field intensity [7]. Many schemes have been proposed to optimally compromise between photon shot noise and quantum back-action [8], which leads to the standard quantum limit (SQL) in weak force sensing [9, 10]. Various approach beyond-SQL measurements have been proposed [11–15], including optical squeezing in the optomechanical system [5, 14], atomic assistance in a separate cavity [13], mechanical modification by the light [15], and so on. Up to now, most of the measurement schemes are based

on the Born-Markov approximation. The noise effect from a structured bath for optomechanical measurement is still not discussed. On the other hand, how to improve detecting precision with a structured bath is also unresolved. Thus, investigation measurement noise under a structured environment is a practical requirement for the further development of high precision measurements.

Generally speaking, the quantal consideration of thermal noise of the optomechanical measurement system can be adequately described as a movable mirror undergoing quantum Brownian motion with the coupling through the reservoir momentum [16]. The dynamics of this system are a non-Markovian process essentially. Since the non-Markovian environment exhibits memory effect [17–21] which can be used to store quantum information [17], to generate and protect entanglement [18, 22] and to enhance the side-band cooling effect [19, 23], it might be beneficial for high precision measurements due to the same requirements of quantum behavior protection. Most recently, a kind of non-Markovian environment for mechanical oscillator had been designed, in which spectrum density of the environment was detected [24], which makes it possible to detect the weak force under a structured environment. With this consideration in mind, we investigate the detection property based on an elementary optomechanical system where the mechanical oscillator is coupled to a non-Markovian reservoir, while the bath of the cavity is a Markovian environment so as to output the signal of oscillator through the cavity.

In this paper, we introduce a non-Markovian environment for the mechanical oscillator and obtain the solution of output signal under homodyne detection. Then we study the sensibility and additional noise of an optomechanical weak force detection system with different spectrum densities $\mathcal{J}(\omega)$ including that of Markovian condition. We find that some environments with super-Ohmic spectrum or experimental cut-off spectrum [24] do have obvious enhanced sensibility comparing with that under Markovian condition. Furthermore, we can greatly reduce the additional noise even in the unsolved sideband regime.

2. Model

We consider a typical optomechanical system where the frequency of the cavity and the mechanical resonator are ω_c and ω_m , respectively. The weak force is sensed by the mechanical oscillator, and the environment noise simultaneously exerts a stochastic force to the oscillator. In order to detect the signal force, we assume that the mechanical oscillator is coupled to a non-Markovian reservoir so as to decrease stochastic force. Considering the feasibility, a Markovian environment for optical mode is easy to output the optical signal to perform homodyne detection in experiment. Therefore, we consider the optical mode in Markovian regime. As shown in Fig. 1, the output signal can be processed in the standard homodyne detection. The Hamiltonian of the system can be

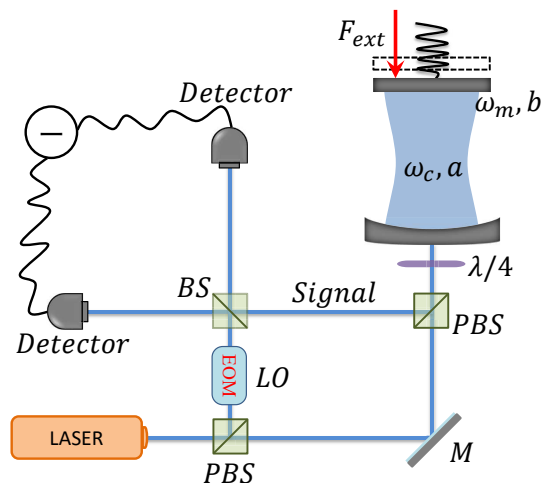


Figure 1. (color online) Schematic of the system with homodyne detection. The local oscillator (LO) is phase-modulated with an electro-optical modulator (EOM). The monitored system is composed of a optomechanical cavity and a general non-Markovian reservoir of the mechanical oscillator.

described as $H = H_S + H_E$ with

$$\begin{aligned}
 H_S &= \hbar\omega_c a^\dagger a + \frac{1}{2}\hbar\omega_m(p_m^2 + q_m^2) - \hbar g_0 a^\dagger a q_m + i\hbar E(a^\dagger e^{-i\omega_d t} - a e^{i\omega_d t}), \\
 H_E &= \sum_k \hbar\omega_k \left[\frac{1}{2}(p_k^2 + q_k^2) + \gamma_k q_k q_m \right],
 \end{aligned} \tag{1}$$

where H_S describes the cavity mode driven by a laser coupled to the mechanical resonator via radiation pressure with the coefficient $g_0 = (\omega_c/L)\sqrt{\hbar/2m\omega_m}$. And ω_d is the angular frequency of the laser, and E is the cavity driving strength given by $E \equiv 2\sqrt{P\kappa_{ex}/\hbar\omega_d}$ with P the input power of the laser and κ_{ex} the input rate of the cavity. The first term of H_E is the energy of the mechanical reservoir for the k th environmental oscillator with frequency ω_k . The second term of H_E describes the coupling between the mechanical oscillator and the reservoir with the coupling strength $\omega_k\gamma_k$ for the k th environmental mode. For convenience, we take $\hbar = 1$ throughout the paper. In the rotating frame at the driving laser frequency ω_d , the time evolution of the system and reservoir operators in the Heisenberg picture are

$$\dot{a} = -\left(i\Delta_c + \frac{\kappa}{2}\right)a + ig_0 a q_m + E + \sqrt{\kappa} a_{in}, \tag{2a}$$

$$\dot{q}_m = \omega_m p_m, \tag{2b}$$

$$\dot{p}_m = -\omega_m q_m + g_0 a^\dagger a - \sum_k \omega_k \gamma_k q_k, \tag{2c}$$

$$\dot{q}_k = \omega_k p_k, \tag{2d}$$

$$\dot{p}_k = -\omega_k q_k - \omega_k \gamma_k q_m, \tag{2e}$$

where $\Delta_c = \omega_c - \omega_d$, κ and a_{in} denote the dissipation rate and noise operator of the cavity, respectively. The autocorrelation function of the vacuum noise is $\langle a_{in}(t)a_{in}^\dagger(\tau) \rangle =$

$\delta(t - \tau)$. Solving Eqs. (2d) and (2e), we have

$$q_k(t) = q_k(0) \cos(\omega_k t) + p_k(0) \sin(\omega_k t) - \omega_k \gamma_k \int_0^t d\tau q_m(\tau) \sin[\omega_k(t - \tau)]. \quad (3)$$

Substituting it into Eq. (2c),

$$\dot{p}_m = -\omega_m q_m + g_0 a^\dagger a + \int_0^t d\tau f(t - \tau) q_m(\tau) + F_{in},$$

where $f(t) = \sum_k \omega_k^2 \gamma_k^2 \sin \omega_k t = \int \frac{d\omega}{2\pi} \mathcal{J}(\omega) \sin \omega t$. $F_{in} = F_{ext} + \xi(t)$, here $\xi(t) = -\sum_k \omega_k \gamma_k [q_k(0) \cos(\omega_k t) + p_k(0) \sin(\omega_k t)]$ is the input-noise of the oscillator, which depend on the initial states of the reservoir. In Markovian regime this term is usually written as $\sqrt{\gamma_m} F_{th}$, where γ_m is the dissipation rate of the mechanics, and F_{th} is the noise operator. F_{ext} is the external forces to be measured [13, 14], which can be a accelerated mass [25], magnetostrictive material [26], atomic force [27] or gravitational waves [28]. Currently, most experimental realizations of cavity optomechanics are still in the single-photon weak coupling with strong driving condition [29–32]. Under this condition, we can linearize the equations of motion around the steady state with $p_m \rightarrow p_m + p_0$, $q_m \rightarrow q_m + q_0$, $a \rightarrow \alpha + a$, here $p_0 \equiv \langle p_m \rangle$, $q_0 \equiv \langle q_m \rangle$ and $\alpha \equiv \langle a \rangle$. Neglecting the nonlinear term, we write the linearized quantum Langevin equations as

$$\begin{aligned} \dot{a} &= -\left(i\Delta'_c + \frac{\kappa}{2}\right)a + iGq_m + \sqrt{\kappa}a_{in}, \\ \dot{q}_m &= \omega_m p_m, \\ \dot{p}_m &= -\omega_m q_m + \int_0^t d\tau f(t - \tau) q_m(\tau) + G^*a + Ga^\dagger + F_{in}, \end{aligned} \quad (4)$$

where $G = \alpha g_0$ is the linearized coupling strength, $\Delta'_c = \Delta_c - g_0 q_0$ denotes the effective detuning of the cavity. In order to solve the dynamics of the system and to find the input noise sources, we now switch into the frequency domain by introducing the Fourier transform operator $O(\omega) = \frac{1}{\sqrt{2\pi}} \int dt O(t) e^{i\omega t}$ and obtain

$$\begin{aligned} a(\omega) &= \chi_c(\omega) [iGq_m(\omega) + \sqrt{\kappa}a_{in}(\omega)], \\ q_m(\omega) &= \chi_m(\omega) [G^*a(\omega) + Ga^\dagger(-\omega) + F_{in}(\omega)], \end{aligned} \quad (5)$$

where $\chi_c \equiv [\kappa/2 - i(\omega - \Delta'_c)]^{-1}$ and $\chi_m \equiv -\omega_m / [(\omega^2 - \omega_m^2) + \omega_m \Sigma(\omega)]$ are susceptibilities of cavity and mechanical oscillator with $\Sigma(\omega) = \mathcal{P} \int d\omega' \frac{\omega' \mathcal{J}(\omega')}{(\omega^2 - \omega'^2)} \mp i\pi \frac{\theta(\omega) \mathcal{J}(\omega) - \theta(-\omega) \mathcal{J}(-\omega)}{2}$ the Laplace transform of the self-energy correction [18, 33], where $\theta(\omega)$ is a step function. Here χ_m denotes the effect of the mechanical bath which depends on the spectrum density $\mathcal{J}(\omega)$. The commonly used ohmic-type spectral density of the form $\mathcal{J}(\omega) = \eta \omega \left(\frac{\omega}{\omega_0}\right)^{s-1} e^{-\frac{\omega}{\omega_0}}$ [33–35], where η is the strength of system-bath coupling, and ω_0 is the cut-off frequency. The exponent s is a real number that determines the ω dependence of $\mathcal{J}(\omega)$ in the low-frequency region. The baths with $0 < s < 1$, $s = 1$, and $s > 1$ are termed as “sub-Ohmic”, “Ohmic” and “super-Ohmic” baths, respectively. In Markovian condition $\chi_m = -\omega_m / [(\omega^2 - \omega_m^2) + i\gamma_m \omega]$, where γ_m is the dumping rate of the mechanical oscillator. Similarly, in non-Markovian regime we can also define the

equivalent dissipation rate γ_{eff} which depends on the spectrum density $\mathcal{J}(\omega)$. Solving Eq. (5), we have

$$q_m(\omega) = \frac{G^* \chi_c \sqrt{\kappa} a_{in}(\omega) + G \chi'_c \sqrt{\kappa} a_{in}^\dagger(-\omega) + F_{in}(\omega)}{\chi_m^{-1} - i|G|^2(\chi_c - \chi'_c)}, \quad (6)$$

where $\chi'_c = [\kappa/2 - i(\omega + \Delta'_c)]^{-1}$. In Eq. (6) the coordinate of mechanical operator in frequency domain is composed of two parts. The one term is proportion to the input field of the cavity through the radiation pressure coupling with the coefficient G . The other term $F_{in}(\omega)$ is resulted from the bath of the oscillator and external force. If we neglect the effect from the cavity, we can rewrite Eq. (6) as $q_m(\omega) = \chi_m(\omega) F_{in}$. There is an obvious positive correlation between the external force and the position spectrum of the oscillator. For weak force detection, we need a large susceptibility $\chi_m(\omega)$ to magnify the weak signal F_{ext} . On the other hand, the thermal noise from the environment should be reduced, because the noise can be coequally amplified with the detecting signal by the system. In Markovian regime, the two requirements will demand a high mechanical quality factor and low bath temperature [1]. But it is more complex in non-Markovian condition, $\chi_m(\omega)$ totally depends on the self-energy correction $\Sigma(\omega)$ which is a frequency dependent parameter up to the structure of the bath. We will make a specific discuss in the follow section.

It is hard for us to direct detect the oscillator experimentally. But the signal from the external force can be output and enhanced by the cavity through the optomechanical interaction. Usually, we use the output photon from the optomechanical cavity as an indirect information carrier. Under Markovian regime for the optical field, we can use the standard input-output relation $O_{out} = \sqrt{\kappa} O - O_{in}$. Considering a homodyne measurement shown in Fig. 1, we have the signal

$$\begin{aligned} M_{out}(\omega) &= i[a_{out}^\dagger(-\omega)e^{-i\theta} - a_{out}(\omega)e^{i\theta}] \\ &= A(\omega)a_{in}(\omega) + B(\omega)a_{in}^\dagger(-\omega) + C(\omega)F_{in}, \end{aligned} \quad (7)$$

where

$$\begin{aligned} A(\omega) &= \frac{4e^{i\theta}\kappa G^{*2}\chi_m - ie^{-i\theta}[D(4|G|^2\chi_m - D) + 4\omega^2]}{\sqrt{2}[4\Delta'_c(\Delta'_c - 2|G|^2\chi_m) + (\kappa - 2i\omega)^2]}, \\ B(\omega) &= \frac{4e^{-i\theta}\kappa G^2\chi_m + ie^{i\theta}[D^*(4|G|^2\chi_m - D^*) + 4\omega^2]}{\sqrt{2}[4\Delta'_c(\Delta'_c - 2|G|^2\chi_m) + (\kappa - 2i\omega)^2]}, \\ C(\omega) &= \frac{2i\sqrt{\kappa}\chi_m[e^{i\theta}G^*(D^* - 2\omega) - e^{-i\theta}G(D + 2\omega)]}{\sqrt{2}[4\Delta'_c(\Delta'_c - 2|G|^2\chi_m) + (\kappa - 2i\omega)^2]}, \end{aligned} \quad (8)$$

with $D = 2\Delta'_c + i\kappa$, and the phase θ is introduced and can be optimized to enhance the sensitivity of the weak force detection [14]. To obtain the relationship between the detecting force and the output signal, we can rewrite Eq. (7) as

$$\frac{M_{out}(\omega)}{C(\omega)} = \frac{A(\omega)}{C(\omega)}a_{in}(\omega) + \frac{B(\omega)}{C(\omega)}a_{in}^\dagger(-\omega) + F_{in}. \quad (9)$$

Considering $F_{in} = F_{ext} + \xi(\omega)$ and defining $M_{out}(\omega)/C(\omega) = F_{ext} + F_{add}(\omega)$, then we have

$$F_{add} = \xi(\omega) + \frac{A(\omega)}{C(\omega)}a_{in}(\omega) + \frac{B(\omega)}{C(\omega)}a_{in}^\dagger(-\omega), \quad (10)$$

where F_{add} is the additional noise of the detecting force. The first term denotes the thermal noise operator of the mechanical environment, and the second and third term denote the input noise of the cavity. From the general definition of the noise spectrum, we have

$$S_{add}(\omega) = \frac{1}{2}[S_{FF}(\omega) + S_{FF}(-\omega)], \quad (11)$$

where $S_{FF}(\omega) = \int d\omega' \langle F_{add}(\omega)F_{add}(\omega') \rangle$. Here we assume that any two parts initially have no correlation. The vacuum radiation input noise a_{in} satisfy δ -correlation function. The additional noise spectrum density becomes

$$S_{add}(\omega) = S_{\xi\xi}(\omega) + \frac{|A(\omega)|^2 + |B(\omega)|^2}{2|C(\omega)|^2}, \quad (12)$$

where $S_{\xi\xi}(\omega)$ is thermal noise with the structured bath which does not depended only on the bath temperature but also on the spectrum density $\mathcal{J}(\omega)$. For simplicity, we choose $\theta = 0$, then Eq. (12) can be rewritten as

$$S_{add}(\omega) = S_{\xi\xi}(\omega) + \frac{|P(\omega)|^2 + |Q(\omega)|^2}{8\kappa|G^*D^* - GD - 2\omega(G + G^*)|^2}. \quad (13)$$

where

$$\begin{aligned} P(\omega) &= 4(\kappa G^{*2} - iD|G|^2) + \frac{i(D^2 - 4\omega^2)}{\chi_m} \\ Q(\omega) &= 4(\kappa G^2 + iD^*|G|^2) - \frac{i(D^{*2} - 4\omega^2)}{\chi_m} \end{aligned} \quad (14)$$

$S_{add}(\omega)$ is also defined as a effective force noise spectral density to evaluate the sensitivity to the external force [14]. We will show that the effective force noise can be reduced by engineering the environment.

3. The mechanical susceptibility and thermal correlation with a structured environment

Before we investigate the additional noise spectrum, we first analyze the effect of the ability of amplification $\chi_m(\omega)$ and thermal noise spectrum $S_{\xi\xi}(\omega)$ under non-Markovian environment. As we have mentioned in last section, the sensibility of the mechanical oscillator for the weak force ultrasensitive detection in optomechanical system is determined by the quantity $\chi_m(\omega)$ and has been widely discussed in Markovian regime [36,37]. In non-Markovian regime, $\chi_m(\omega)$ is a spectrum depended parameter. According to (6), considering the effect of cavity, we now present the character of mechanical susceptibility by plotting $\chi_{xm}(\omega)/\chi_{x0}$ as a function of ω with the commonly used ohmic-type spectrum in Fig. 2a and b, where $\chi_{xm}^{-1} = \chi_m^{-1} - i|G|^2(\chi_c - \chi'_c)$ denote the mechanical

sensitivity, $\chi_{x0}^{-1} = -i\gamma_{eff} - i|G|^2[\chi_c(\omega_m) - \chi'_c(\omega_m)]$ is optimal mechanical sensitivity in Markovian regime. As shown in Fig. 2a, it is clearly seen that the maximal sensitive frequency area is around the oscillator frequency ω_m in Markovian regime, which is consistent with the generally results in weak force detection in Ref. [1]. For ohmic-type spectrum, super-Ohmic environment could provide an obviously amplification for susceptibility of detection. We also notice that, a structured bath will cause a frequency displacement of the maximal susceptibility, because ω_m is substituted by the effective frequency $\omega_{eff} \approx \sqrt{\omega_m[\omega_m + \mathcal{P} \int d\omega' \frac{\omega' \mathcal{J}(\omega')}{(\omega_m^2 - \omega'^2)]}$ for a structured reservoir [18]. And the optimal detection area should be on resonance with this effective frequency (Resonance Amplification).

In Fig. 2b, we plot the maximal ratio of mechanical sensitivity $\chi_{xm}(\omega)/\chi_{x0}$ with different environment as a function of dumping rate γ_{eff} . Here γ_{eff} is a spectrum depended parameter which describes the dissipation strength of the structured bath, through the inverse Laplace transform of $\Sigma(\omega)$ we have $\gamma_{eff} \approx \pi \mathcal{J}(\omega_m)$ [38]. Under this condition, γ_{eff} proportion to the system-bath coupling strength η . It is shown that, for ohmic-type spectrum, the maximal ratio of mechanical sensitivity $\chi_{xm}(\omega)/\chi_{x0}$ exhibits vibration behavior with the increase of effective dissipation rate γ_{eff} . The maximal sensitivity ratio of the system will reach the peak value at some specific effective dissipation rate γ_{eff} , and does not require the system-environment coupling factor η is too strong. Thus, we can significantly enhance the sensitivity with a structured environment, and the corresponding detection frequency should also be modulated.

The thermal noise $S_{\xi\xi}(\omega)$ as background noise negatively affects the weak force detection. In order to improve the precision of the weak force detection, we should reduce the effect result from the thermal noise of the bath of the oscillator. We consider a movable mirror undergoing quantum Brownian motion reservoir. The thermal-noise spectral density is defined as $S_{\xi\xi}(\omega) \equiv \int_{-\infty}^{+\infty} dt e^{i\omega t} \langle \xi(t) \xi(0) \rangle$. Considering the structure of the environment, we have

$$S_{\xi\xi}(\omega) = \int_{-\infty}^{+\infty} dt e^{i\omega t} \int_0^{\infty} d\omega' \mathcal{J}(\omega') [n_{th}(\omega') \cos(\omega' t) + \frac{1}{2} e^{-i\omega' t}], \quad (15)$$

where $n_{th}(\omega) = (e^{\frac{\hbar\omega}{k_B T}} - 1)^{-1}$ is phononic distribution function of the reservoir. $\mathcal{J}(\omega)$ describes the character of the reservoir. For Born-Markov approximation where the system-reservoir coupling rate is weak and the interaction time is short enough, the environment can be described as a flat spectrum and the integral for ω is a delta function of time; therefore, the environment present no memory effect for the system, i.e. $S_{\xi\xi} = \gamma_m n_{th}(\omega_m)$, where γ_m is the dumping rate of the mechanical oscillator, $n_{th}(\omega_m)$ describes the equivalent thermal occupation which is independent of the environment frequency.

As shown in Fig. 2c, we plot the thermal noise spectral density for Markovian and non-Markovian environment as a function of ω . For the exponent $s = 0.5, 1, 2$ the corresponding coupling strength of system-bath for sub-Ohmic, Ohmic and super-Ohmic are $\eta_{0.5} = 5.5 \times 10^{-3}$, $\eta_1 = 1.2 \times 10^{-2}$ and $\eta_2 = 6.1 \times 10^{-2}$, respectively, when we choose

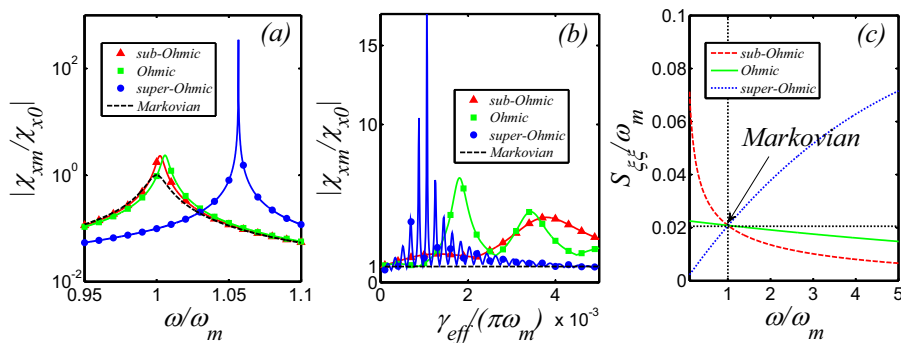


Figure 2. (Color online) (a) The ratio of mechanical sensibility χ_{xm}/χ_{x0} as a function of ω with Markovian condition and ohmic-type spectrum. $s = 0.5, 1, 2$ for three kinds of ohmic-type spectrum, respectively, the equivalent dumping rate $\gamma_{eff}/\omega_m = \pi \times 10^{-3}$. (b) The maximal ratio of mechanical sensibility χ_{xm}/χ_{x0} as a function of equivalent dumping rate γ_{eff} for different spectrum. (c) Thermal noise with three kind of ohmic-type spectrum density. In Markovian regime, the noise exist only at the frequency ω_m , the directrix is plotted by black dashed line, while $s = 0.5$ for sub-Ohmic spectrum, $s = 1$ for Ohmic spectrum, $s = 2$ for super-Ohmic spectrum. The equivalent dissipation $\gamma_{eff} = \pi \times 10^{-3}\omega_m$. Other parameters are, the oscillator frequency $\omega_m = 10^6 Hz$, the bath temperature $T = 1mK$, the cut-off frequency $\omega_0/\omega_m = 10$.

the same equivalent dumping rate $\gamma_{eff} = \pi \times 10^{-3}\omega_m$ as that for Markovian condition. For a fair comparison, the other parameters are also selected the same for different structured bath. From Fig. 2c, we see that different structure of bath will cause different distribution of thermal excitation. But, around frequency ω_m , $S_{\xi\xi} \approx 0.02$ for different reservoir. While the effective frequency ω_{eff} just shifts slightly, we can reasonably ignore the thermal noise $S_{\xi\xi}$ because one can observe that $S_{\xi\xi}$ is below 0.025 around ω_m . Under Markovian reservoir, according to Eq. (15), for the common used detection frequency area ω_m , the noise $S_{\xi\xi} \approx \gamma_{eff} \frac{k_b T}{\hbar \omega_m} = k_b T / (\hbar Q_{eff})$. Thus we can reduce the thermal noise by cooling down the system [19] or improve the effective mechanical quality factor Q_{eff} directly. According to the experiment parameters in nano-mechanical system [12], where $\omega_m = 2\pi \times 1.04MHz$, mechanical quality factor $Q_m = 6.2 \times 10^5$ and the environment temperature $T = 77mK$, the thermal noise $S_{\xi\xi}/\omega_m \ll 1$, which means that we can ignore the thermal noise for weak force detection under current experimental conditions [6].

4. The additional noise with a structured environment

For weak force detection, in addition to a high sensitivity, good linearity and high response speed, we expect to reduce additional noise, which is also widely used as a detection waveband, such as weak force detection through OMIT [39], microwave quantum illumination by optomechanical system [3], gravitational-wave detectors with unstable optomechanical filters [28]. Now, we show that under certain environment we can obtain high sensitivity and reduced additional noise.

Recently, a spectral density of mechanical environment had been detected

experimentally through the emitted light of micro-optomechanical system [24]. The demonstration device consists of a thick layer of Si_3N_4 with a high-reflectivity mirror pad in its centre as a mechanically moving end mirror in a Fabry-Pérot cavity where the spectral density is described by $\mathcal{J}(\omega) = C\omega^k$ with $C > 0$ and $k = -2.30 \pm 1.05$. The region of ω satisfies $\omega \in [\omega_{min}, \omega_{max}]$ centred around mechanical resonance frequency $\omega_m = 914kHz$. Here $\omega_{min} = 885kHz$ and $\omega_{max} = 945kHz$, the corresponding bandwidth $\Gamma \approx 0.07\omega_m$. Employing this cut-off experimental spectral density $\mathcal{J}(\omega) = C\omega^k$, where $C = \mathcal{J}(\omega_m)/\omega_m^k$, and we choose the bandwidth $\Gamma_m = 0.2\omega_m$, exponent $k = -2$.

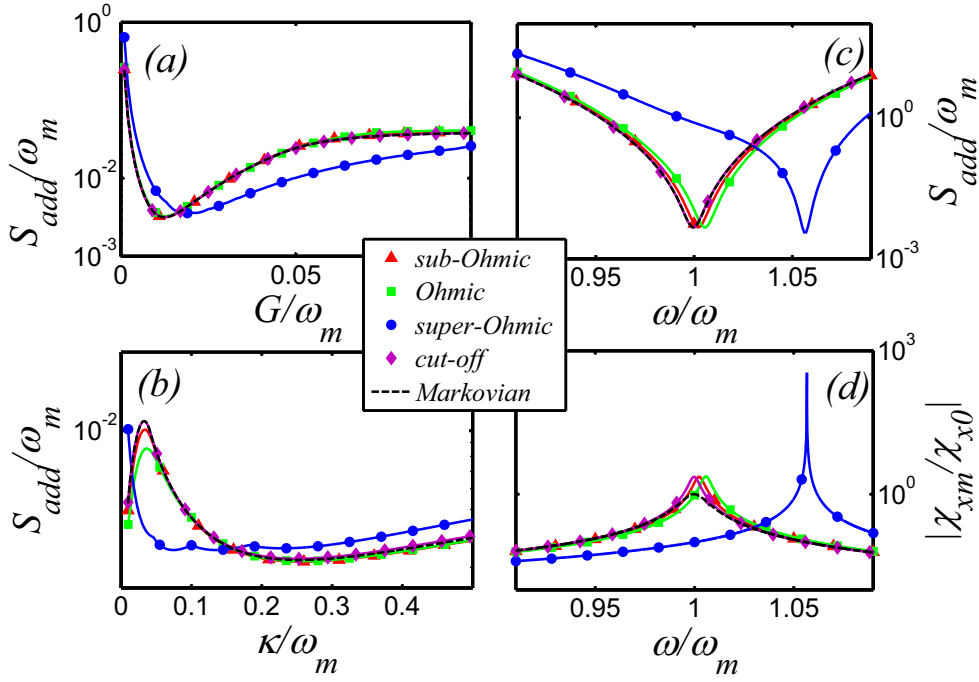


Figure 3. (Color online) (a), (b) and (c) describe the optimal additional noise S_{add} as a function of linearized coupling rate G , dissipation rate κ and frequency ω , respectively. (a) The dissipation rate $\kappa/\omega_m = 0.1$. (b) The linearized coupling rate $G/\omega_m = 0.02$. (c) The dissipation rate $\kappa/\omega_m = 0.1$ and linearized coupling rate $G/\omega_m = 0.02$. (d) The ratio of mechanical susceptibility χ_{xm}/χ_{x0} as a function of ω with different spectrum. The equivalent damping rate $\gamma_{eff}/\omega_m = \pi \times 10^{-3}$. Other parameters are same with Fig. 2.

We plot the additional noise and the susceptibility for the different types of environment of the mechanical oscillator in Fig. 3, where we reasonably ignore thermal noise $S_{\xi\xi}$ around ω_m [6] in Eq. (13) according to the conclusion in Sec. 3. As shown in Fig. 3a, we plot the optimal additional noise S_{add} as a function of linearized coupling rate G . It is obvious that for different spectrum, there are minimum values of S_{add} at certain value of G . In addition to the super-Ohmic spectrum, the evolution trend of the curve with the coupling rate G is almost the same. When the coupling rate G/ω_m is less than 0.017, the additional noise of the super-Ohmic spectrum is larger than that of other ones. On the contrary, the additional noise of the super-Ohmic spectrum will be less

than that of other spectrums. In the large G scale, the additional noise is independent of the structure of the environment. Under this region, the additional noise mainly governed by the vacuum fluctuations of the cavity through optomechanical interaction, and the noise from the mechanical environment can be ignored. Thus, in order to reduce the additional noise the driving strength of the cavity should not be too strong.

In Fig. 3b, we plot the optimal additional noise S_{add} as a function of damping rate κ which can be adjusted by Q-technology in the measurement [40]. As shown in Fig. 3b, in addition to the super-Ohmic spectrum, evolution curve of the additional noise with the dissipation rate κ tends to be consistent. There is a peak value of the additional noise at the specific dissipation rate κ . With the increase of the dissipation rate, the additional noise decreases first and then increases gradually. For the super-Ohmic spectrum, when the dissipation rate κ/ω_m is less than a specific value 0.16, the additional noise is much smaller than that of other structures. With the increase of the dissipation rate, the additional noise of the super-Ohmic spectrum will be larger than that of other ones. In resolved sideband regime, the additional noise of the system for different spectral structures can be maintained at a low level 10^{-3} . That is to say, in the weak dissipation region, the super-Ohmic spectrum can effectively reduce the additional noise. However, there is no obvious effect on reducing the additional noise for other spectral structures under the same effective dissipation γ_{eff} .

Employing the optimized parameters based on Figs. 3a and 3b, we plot the additional detection noise and sensitivity in frequency region shown in Figs. 3c and 3d. The additional noise S_{add}/ω_m can be reduced to near 10^{-3} at the effective frequency ω_{eff} . The mechanical sensitivity of the system has been significantly improved for the ohmic-type spectrum. Especially for the super-Ohmic spectrum, the sensitivity is about 10^3 times of Markovian condition.

Comparing Fig. 3c and Fig. 3d, one can observe that the frequency region with minimum detection noise is exactly the frequency region with optimal sensibility. As shown in the numerator of the second term of Eq.(13) and Eq.(14), the maximal sensibility $|\chi_m|$ results in the optimal S_{add} (Because D is independent with frequency ω). Thus, in our scheme, we can detect the weak force with maximal sensibility and minimum additional noise.

Considering the feasibility, we can easy to adjust the rate G/ω_m by controlling the driving power of the cavity so as $G/\omega_m < 0.05$ (see Fig. 3a). Since the *cut-off* spectrum [24] has been realized in experiment, we can employ it to reduce the addition noise even in the unsolved sideband regime which shows in Fig. 3b. In order to maintain the coherence, the low-loss rate of the mechanical oscillator is still needed.

5. Force sensing in general environment

In order to show the advantages of the detection under non-Markovian environment. We provide an example to measure the mass of the human chromosome-1. The mass of one chromosome-1 molecule is about $2.7 \times 10^{-13}\text{g}$ [41]. The external accretion mass

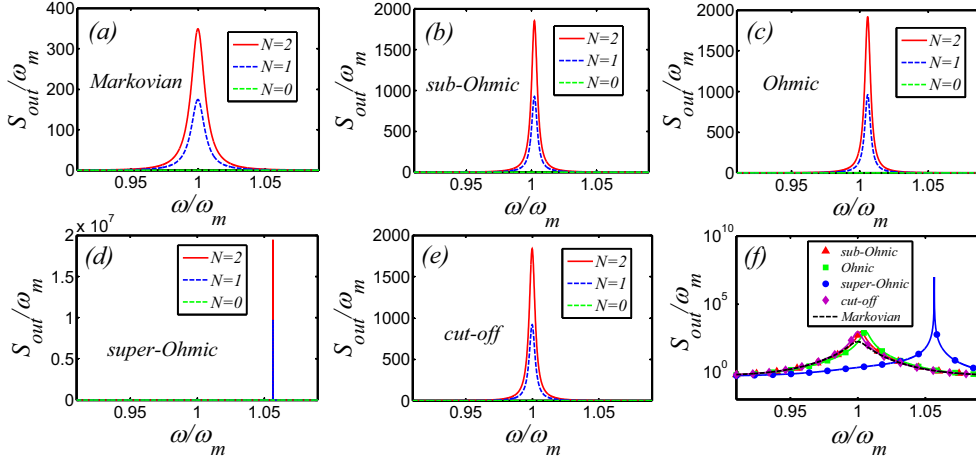


Figure 4. The output signal $S_{out}(\omega)$ as function of frequency ω after landing the chromosomes ($N = 0, 1, 2$) with the bath type of (a) Markovian condition, (b) sub-Ohmic spectrum, (c) Ohmic spectrum and (d) super-Ohmic spectrum. (e) Experimental cut-off spectrum. (f) Comparison of different spectral structure of output signal with $N = 1$. Other parameters are same with Fig. 2.

will introduce an additional frequency responded by mechanical resonator. The mass response of the mechanical resonator can be defined as $\mathcal{R} = \partial\omega/\partial m$ with the typical value $\mathcal{R} = 10^{21} \text{ Hz} \cdot \text{g}^{-1}$ [42, 43]. Then, we deposit a few chromosomes onto the surface of the mechanical resonator and observe the output signal of the system. As shown in Fig. 4, we plot the output signal $S_{out}(\omega)$ (details see Appendix) of the optomechanical mass sensor with differently structured environment. For fair comparison, we choose the same effective dissipation rates as well as optomechanical cavity parameters for different environments. From Fig. 4a to 4e, we can see that the energy of the output spectrum of the resonance frequency increases as the number of adsorbed chromosomes increases. That is to say, we can detect the number of the chromosomes by measuring the strength of the resonant output energy $I_{out} = S_{out}(\omega_{eff})$. By comparing the Markovian condition, ohmic-type spectrums and experimental cut-off spectrum in Fig. 5f, we find that the detection energy response is enhanced while the noise is reduced (the bandwidth is narrowed) for the ohmic-type and cut-off spectrum. Especially for super-Ohmic spectrum, the energy response of mass detection is almost 5×10^4 times of the Markovian condition's. This conclusion is similar to what we discussed in the previous section: we can detect the weak force with maximal sensibility and minimum additional noise in specific non-Markovian environment.

As shown in Fig. 5a, there is a significant linear relationship between the resonance response energy I_{out} and the number of the chromosomes N . Therefore, our scheme totally consistent with the basic requirements of weak force detection. As shown in Fig. 5b, by comparing two different conditions, we can see that the output energy of the detection can be concentrated in a small area around the effective frequency ω_{eff} due

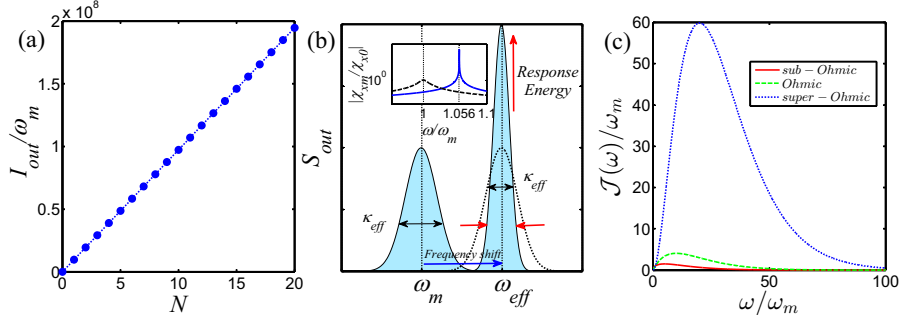


Figure 5. (a) The linear relationship between the resonance response energy I_{out} and the number of the chromosomes N in super-Ohmic environment. (b) Comparison of output spectrum between Markovian condition (centre around ω_m) and super-Ohmic environment (centre around ω_{eff}). (c) The spectrum of three ohmic-type environment. The parameters are same with Fig. 2.

to the specific structure of the super-Ohmic spectrum. The sensitivity or the response energy of the sensor to the input signal in super-Ohmic environment is much higher than that in Markovian condition, which can be seen in the subgraph of Fig. 5b. As we have chosen the same effective dissipation rate of the oscillator and other parameters of the optomechanical system, the noise energy from the cavity and mechanical environment are the same. So the signal-noise ratio of the mass sensor in super-Ohmic environment is larger than that in Markovian condition while the bandwidth of the output spectrum is narrowed. This process is similar to “squeezing” the response energy of the input signal. We can understand the mechanism of the optimized weak force detection in non-Markovian regime by analyzing the response of the output field to non-Markovian environment. The mechanical oscillator is a sensor of weak force while the external force can be regarded as a part of the mechanical environment undoubtedly. The environment of the sensor affects the weak force detection which can be seen in Fig. 4. Thus, the response of the weak force detection system depended on the coupling effect between the mechanical oscillator and its environment. The only different in the comparison between the Markovian and non-Markovian condition is the characters of the environment structure. In Born-Markov approximation, the environment be equivalent to a flat spectrum. The effective response of the oscillator to the environment is the combination of the average coupling effect of all bath mode and frequency detuning between the mechanical mode and bath mode, which can be seen in the subgraph of Fig. 5b, the response coefficient χ_{xm} is a symmetrical distribution around ω_m . But the system-bath response is depended on the environment spectrum $\mathcal{J}(\omega)$ for structured bath.

In order to understand the reason why the super-Ohmic spectrum is superior to others, we plot Fig. 5c. As shown in Fig. 5c, the $\mathcal{J}(\omega)$ distribution of super-Ohmic spectrum mainly concentrates in the low frequency region (detection region), and the contribution of the high frequency mode of the environment can even be ignored. But the distribution for sub-Ohmic and Ohmic spectrum are more gentle than the super-

Ohmic spectrum. Therefore, we can safely say that the super-Ohmic spectrum are more far away from the flat spectrum of Markovian environment than that for sub-Ohmic and Ohmic spectrum. As we all know, the Markovian environment only contributes a stochastic force. So, it is reasonable that the non-Markovian backaction can reduced the noise. Since the super-Ohmic spectrum is the most different from the Markovian flat spectrum, it can be the best for decreasing noise force. Subgraph in Fig. 5b clearly show that the response coefficient χ_{xm} of super-Ohmic spectrum is much higher than that for the other spectrum in the detection frequency region. In addition, super-Ohmic spectrum of its superiority in decreasing noise [44] over Ohmic and sub-Ohmic spectrum had also been observed in cooling the mechanical oscillator [19]. Therefore, in our scheme, the output signal of the weak force detection could exhibit high response and high sharpness spectrum in non-Markovian regime, which can be implemented to improve the detection accuracy for both energy response sensor [45, 46] and frequency response sensor [41, 47].

In above discussion, the environment of the optical cavity is Markovian. If we would like to introduce non-Markovian environment for the cavity field, the additional term $H_{CE} = \sum_k [\hbar\nu_k b_k^\dagger b_k + i\hbar\mathcal{K}_k(b_k a^\dagger - h.c.)]$ should be added in the Hamiltonian H . Insteadly, Eq. (2a) should be substituted by another two equations, and the output relation also should be renewed. So, the problem become very complicated. It is hard for us to directly foresee the function of the non-Markovian environment of the cavity field. We will finish it elsewhere.

6. Conclusion

We investigate the weak force detection of optomechanical system in non-Markovian regime. By solving the exact dynamics of the optomechanical system, we obtain an general analytical result of the output signal. We have shown that: (i) The thermal noise for weak force detection can be ignored even under non-Markovian environment, while the susceptibility is efficiently amplified in the effective frequency region ω_{eff} . (ii) The additional noise can be significantly reduced in super-Ohmic spectrum. The additional noise can be maintained at a quite low level and the quantum effect can be better protected with a structured bath by comparing with the Markovian condition in resolved sideband regime. (iii) Employing super-Ohmic environment to reduce the additional noise and amplification detection signal do not require the high quality of the cavity. Meanwhile, optimized G/ω_m is demanded. Furthermore, we provide an example by comparing the Markovian and non-Markovian conditions to measure the mass of the human chromosome-1, and then we analyze the mechanism of the optimization detection in non-Markovian regime. Instead of introducing squeezing and improving the experiment conditions such low bath temperature and high mechanical quality factor, our results provides another effective way for reducing the additional noise by utilizing the engineered non-Markovian reservoir in ultrasensitive detection.

7. Acknowledgements

We would like to thank Mr. Wen-Lin Li for helpful discussions. This work was supported by the NSF of China under Grant numbers 11474044 and 11547134.

Appendix A. Output signal of the mass sensor

By using the general definition of the noise spectrum, according to Eq. (7), we can obtain the output signal of the weak force detection system

$$\begin{aligned} S_{out}(\omega) &= [\int d\omega' \langle M_{out}(\omega) M_{out}(\omega') \rangle + \int d\omega' \langle M_{out}(-\omega) M_{out}(-\omega') \rangle] / 2 \\ &= \frac{|A(\omega)|^2 + |B(\omega)|^2}{2} + S_{in}(\omega) |C(\omega)|^2 \end{aligned} \quad (\text{A.1})$$

where $S_{in}(\omega)$ denotes the input signal from the external force F_{ext} after ignoring the thermal noise of mechanical oscillator. Here we intend to measure the mass of the human chromosome-1 as example, where the external accretion mass will introduce an additional frequency responded by mechanical resonator with mass responsivity $\mathcal{R} = 10^{21} \text{Hz} \cdot \text{g}^{-1}$. Then, we deposit a few chromosomes onto the surface of the mechanical resonator. The additional energy of the input signal can be described as $S_{in} = Nm\mathcal{R}$, where $m = 2.7 \times 10^{-13} \text{g}$ is the mass of one chromosome-1 molecule. N is the number of the deposit chromosomes. In the non-Markovian regime, ω_m is replaced by the effective frequency ω_{eff} , and the optimal detection area should be on resonance with this effective frequency. We define the strength of the frequency resonance spectrum $I_{out} = S_{out}(\omega_{eff})$, where $\omega_{eff} = \omega_m$ in the Markovian regime. The energy of I_{out} will be linearly increases as the number of adsorbed chromosomes increases. This allows us could detect the number of the chromosomes by measuring the strength of the resonant output energy.

References

- [1] Pontin A, Bonaldi M, Borrielli A, Cataliotti F S, Marino F, Prodi G A, Serra E and Marin F 2014 *Phys. Rev. A* **89**(2) 023848
- [2] Kolkowitz S, Jayich A C B, Unterreithmeier Q P, Bennett S D, Rabl P, Harris J G E and Lukin M D 2012 *Science (New York, N.Y.)* **335** 1603–6
- [3] Barzanjeh S, Guha S, Weedbrook C, Vitali D, Shapiro J H and Pirandola S 2015 *Phys. Rev. Lett.* **114**(8) 080503
- [4] Meystre P and O Scully M 1983 *Quantum Optics, Experimental Gravity, and Measurement Theory* (New York and London: Plenum Press)
- [5] Peano V, Schwefel H G L, Marquardt C and Marquardt F 2015 *Phys. Rev. Lett.* **115**(24) 243603
- [6] Ma Y, Danilishin S L, Zhao C, Miao H, Korth W Z, Chen Y, Ward R L and Blair D G 2014 *Phys. Rev. Lett.* **113**(15) 151102
- [7] Aspelmeyer M, Kippenberg T J and Marquardt F 2014 *Rev. Mod. Phys.* **86**(4) 1391–1452
- [8] Li W, Jiang Y, Li C and Song H 2016 *Scientific Reports* **6** 31095
- [9] Clerk A A, Devoret M H, Girvin S M, Marquardt F and Schoelkopf R J 2010 *Rev. Mod. Phys.* **82**(2) 1155–1208
- [10] Zhang J, Zhang Y and Yu C S 2015 *Scientific Reports* **5** 11701
- [11] Huang S and Agarwal G S 2010 *Phys. Rev. A* **82**(3) 033811

- [12] Teufel J D, Donner T, Castellanos-Beltran M A, Harlow J W and Lehnert K W 2009 *Nature Nanotechnology* **4** 820 (*Preprint* 0906.1212)
- [13] Bariani F, Seok H, Singh S, Vengalattore M and Meystre P 2015 *Phys. Rev. A* **92**(4) 043817
- [14] Xu X and Taylor J M 2014 *Phys. Rev. A* **90**(4) 043848
- [15] Arcizet O, Briant T, Heidmann A and Pinard M 2006 *Phys. Rev. A* **73**(3) 033819
- [16] Giovannetti V and Vitali D 2001 *Phys. Rev. A* **63**(2) 023812
- [17] Chang K W and Law C K 2010 *Phys. Rev. A* **81**(5) 052105
- [18] Cheng J, Zhang W Z, Zhou L and Zhang W 2016 *Scientific Reports* **6** 23678
- [19] Zhang W Z, Cheng J, Li W D and Zhou L 2016 *Phys. Rev. A* **93**(6) 063853
- [20] Yang C J, An J H, Luo H G, Li Y and Oh C H 2014 *Phys. Rev. E* **90**(2) 022122
- [21] Mu Q, Zhao X and Yu T 2016 *Phys. Rev. A* **94**(1) 012334
- [22] Estrada A F and Pachón L A 2015 *New Journal of Physics* **17** 033038
- [23] Triana J F, Estrada A F and Pachón L A 2016 *Phys. Rev. Lett.* **116**(18) 183602
- [24] Gröblacher S, Trubarov A, Prigge N, Cole G D, Aspelmeyer M and Eisert J 2015 *Nature Communications* **6** 7606
- [25] Guzman Cervantes F, Kumanchik L, Pratt J and Taylor J M 2014 *Applied Physics Letters* **104** 221111
- [26] Forstner S, Prams S, Knittel J, van Ooijen E D, Swaim J D, Harris G I, Szorkovszky A, Bowen W P and Rubinsztein-Dunlop H 2012 *Phys. Rev. Lett.* **108**(12) 120801
- [27] Liu Y, Miao H, Aksyuk V and Srinivasan K 2012 *Opt. Express* **20** 18268–18280
- [28] Miao H, Ma Y, Zhao C and Chen Y 2015 *Phys. Rev. Lett.* **115**(21) 211104
- [29] Gröblacher S, Hammerer K, Vanner M R and Aspelmeyer M 2009 *Nature* **460** 724–727
- [30] Tian L 2013 *Phys. Rev. Lett.* **110**(23) 233602
- [31] Li W, Li C and Song H 2016 *Phys. Rev. E* **93**(6) 062221
- [32] Teufel J D, Donner T, Li D, Harlow J W, Allman M S, Cicak K, Sirois a J, Whittaker J D, Lehnert K W and Simmonds R W 2011 *Nature* **475** 359–363
- [33] Zhang W M, Lo P Y, Xiong H N, Tu M Y and Nori F 2012 *Phys. Rev. Lett.* **109**(17) 170402
- [34] Leggett A J, Chakravarty S, Dorsey A T, Fisher M P A, Garg A and Zwerger W 1987 *Rev. Mod. Phys.* **59**(1) 1–85
- [35] Caruso F, Giovannetti V, Lupo C and Mancini S 2014 *Rev. Mod. Phys.* **86**(4) 1203–1259
- [36] Caniard T, Verlot P, Briant T, Cohadon P F and Heidmann A 2007 *Phys. Rev. Lett.* **99**(11) 110801
- [37] Kleckner D, Marshall W, de Dood M J A, Dinyari K N, Pors B J, Irvine W T M and Bouwmeester D 2006 *Phys. Rev. Lett.* **96**(17) 173901
- [38] Ciccarello F 2015 *Phys. Rev. A* **91**(6) 062121
- [39] Duan Z, Fan B, Stace T M, Milburn G J and Holmes C A 2016 *Phys. Rev. A* **93**(2) 023802
- [40] Liu Y C, Xiao Y F, Luan X and Wong C W 2013 *Phys. Rev. Lett.* **110**(15) 153606
- [41] He Y 2015 *Applied Physics Letters* **106** 121905
- [42] Lassagne B, Garcia-Sanchez D, Aguasca A and Bachtold A 2008 *Nano Letters* **8** 3735–3738
- [43] Yang Y T, Callegari C, Feng X L, Ekinici K L and Roukes M L 2006 *Nano Letters* **6** 583–586
- [44] Xiong H N, Lo P Y, Zhang W M, Feng D H and Nori F 2015 *Scientific Reports* **5** 13353
- [45] Brahmns N, Botter T, Schreppler S, Brooks D W C and Stamper-Kurn D M 2012 *Phys. Rev. Lett.* **108**(13) 133601
- [46] Singh V, Shevchuk O, Blanter Y M and Steele G A 2016 *Phys. Rev. B* **93**(24) 245407
- [47] Naik a K, Hanay M S, Hiebert W K, Feng X L and Roukes M L 2009 *Nature nanotechnology* **4** 445–450